Oral Particle Uptake and Organ Targeting Drives the Activity of Amphotericin B Nanoparticles

Dolores R. Serrano[a], Aikaterini Lalatsa[b], M. Auxiliadora Dea-Ayuela[c], Pablo E. Bilbao-Ramos[d], Natalie L. Garrett[e], Julian Moger[e], Josep Guarro[f], Javier Capilla[f], M. Paloma Ballesteros[a], Andreas G. Schätzlein[g], Francisco Bolás[d], Juan J. Torrado[a], Ijeoma F. Uchegbu[g,*]

[a]Departamento de Farmacia y Tecnologia Farmaceutica, Facultad de Farmacia, Universidad Complutense de Madrid, Plaza Ramon y Cajal s/n, Madrid, 28040, Spain.

[b]School of Pharmacy and Biomedical Sciences, University of Portsmouth, St. Michael's Building, White Swan Road, Portsmouth PO1 2DT, UK

[c]Departamento de Farmacia, Facultad de Ciencias de la Salud, Universidad Cardenal Herrera-CEU, Moncada, Valencia, 46113, Spain.

[d]Departamento de Parasitologia. Facultad de Farmacia, Universidad Complutense de Madrid, Plaza Ramon y Cajal s/n, Madrid, 28040, Spain.

[e]School of Physics, University of Exeter, Stocker Road, Exeter, EX4 4QL, UK

[f]Facultat de Medicina, IISPV, Universitat Rovira i Virgili, Sant Llorenç 21, Reus, 43201, Spain

[g]UCL School of Pharmacy, 29-39, Brunswick Square, London, WC1N 1AX, UK.

***Corresponding author**

Postal address: Department of Pharmaceutics, UCL School of Pharmacy, 29-39, Brunswick Square, London, WC1N 1AX, UK.

Email address: ijeoma.uchegbu@ucl.ac.uk;

Tel: +44 207 753 5997

Fax: +44 207 753 5942.

Abstract

There are very few drug delivery systems that target key organs via the oral route, as oral delivery advances normally address gastrointestinal drug dissolution, permeation and stability. Here we introduce a nanomedicine, in which nanoparticles, while also protecting the drug from gastric degradation, are taken up by the gastrointestinal epithelia and transported to the lung, liver and spleen, thus selectively enhancing drug bioavailability in these target organs and diminishing kidney exposure (relevant to nephrotoxic drugs). Our work demonstrates, for the first time, that oral particle uptake and translocation to specific organs may be used to achieve a beneficial therapeutic response. We have illustrated this using amphotericin B, a nephrotoxic drug encapsulated within N-palmitoyl-N-methyl-N,N-dimethyl-N,N,N-trimethyl,6-O-glycolchitosan (GCPQ) nanoparticles and have evidenced our approach in three separate disease states (visceral leishmaniasis, candidiasis and aspergillosis) using industry standard models of the disease in small animals. The oral bioavailability of AmB-GCPQ nanoparticles is 24%. In all disease models, AmB-GCPQ nanoparticles show comparable efficacy to parenteral liposomal AmB (Ambisome®). Our work thus paves the way for others to use nanoparticles to achieve a specific targeted delivery of drug to key organs via the oral route. This is especially important for drugs with a narrow therapeutic index.

Keywords

Amphotericin B, oral delivery, N-palmitoyl,N-methyl,N,N-dimethyl,N,N,N-trimethyl,6-O-glycol chitosan, nanoparticles, nanomedicine

Graphical abstract

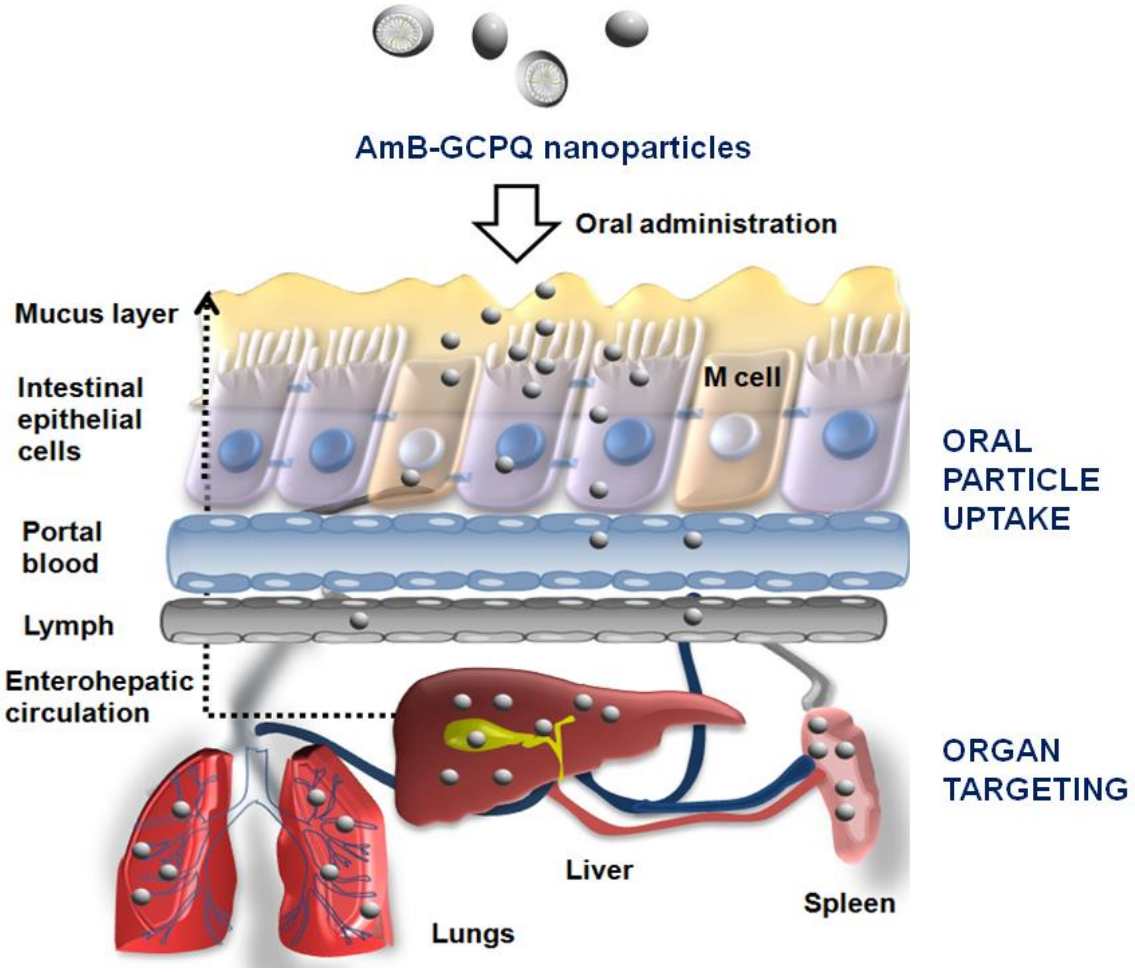

1. Introduction

The oral administration of medicines is a preferred route of administration although a significant proportion of drugs are not orally bioavailable due to their physical properties, an issue which contributes to 40% of drug development failures [1]. An industry, such as the pharmaceutical industry, which experiences 90% of clinical stage failures [2] and thus has to spend upwards of US$ 1 billion to develop a single new chemical entity medicine, requires new technologies that will enable medicine administration via the preferred route, regardless of the chemical features of any promising compounds. Oral drug delivery advances, to date, have focused on gastrointestinal drug dissolution [3], gastrointestinal drug permeability [4] and gastrointestinal compound stability [5].There are no technologies which have as their goal specific organ targeting via the oral route. Our central hypothesis is that nanoparticles which target specific organs via the oral route will confer oral activity on drugs which are not otherwise active through this route. Targeting particular organs of pathology and avoiding sites of toxicity is the goal of drug delivery. Here we present a nanoparticle system that allows oral targeting to the organs of pathology, i.e. the lung, liver and spleen, via the oral route but avoids delivery to the organs of toxicity, the kidneys. Such a system will be of particular relevance to nephrotoxic drugs. The utility of the system is illustrated via the use of amphotericin B (AmB), one of the most effective antifungal drugs used for the treatment of life-threatening systemic fungal infections such as candidiasis or aspergillosis and a drug that is also indicated for the treatment of visceral leishmaniasis [6, 7]; the latter due to its very high cure rate and near absence of resistance. Intravenous administration of AmB marketed formulations (Fungizone®, Ambisome®, Abelcet® and Amphocil®) results in high drug levels in the target organs, i.e. the liver, spleen and lungs but also results in drug accumulation in the kidney, leading to toxicity,

as the drug is nephrotoxic. Both nephrotoxicity and infusion-related side effects, such as infections, thrombophlebitis, fever, chills, vomiting, headaches and haemolysis limit the usefulness of parenteral AmB formulations. Furthermore, the requirement for hospitalisation during treatment, hampers access to parenteral AmB, especially in low resource environments such as developing countries [7, 8]. To date, no oral AmB formulations have been marketed because of AmB's poor gastrointestinal solubility and permeability [9, 10]. Therefore, developing an oral AmB formulation is a viable means of improving patient access to treatment worldwide.

N-palmitoyl-N-monomethyl-N,N-dimethyl-N,N,N-trimethyl-6-O-glycolchitosan (GCPQ) is a self-assembling nanoparticle forming polymer that is taken up by enterocytes and enables the bioavailability of hydrophobic drugs and peptides[11-14]. Our oral drug organ targeting hypothesis will be tested by encapsulating AmB in GCPQ nanoparticles and studying drug and particle biodistribution and drug pharmacological efficacy in comparison to control nanoparticle systems: i.e., AmB liposomes (Ambisome®) or AmB deoxycholate micelles (AMBd).

2. Experimental section

2.1. Polymer synthesis and characterization

GCPQ and deuterated GCPQ were synthesized and characterised as previously described[11-13, 15, 16]. Nuclear Magnetic Resonance (^{1}H NMR) experiments were performed to determine the degree of substitution of the polymer. The level of palmitoylation was calculated as the ratio between palmitoyl methyl protons *(*δ= 1.30-1.40) and sugar methine/methylene protons *(*δ= 3.5-4.5). The level of quaternization was calculated based on the ratio of quaternary ammonium methyl protons (δ= 3.4) to sugar methine/methylene protons *(*δ= 3.5-4.5). The Hydrophobicity Index (HI) was calculated as the ratio between palmitoylation (mole %) and quaternary ammonium groups (mole%). Gel Permeation Chromatography- Multiangle Laser Light Scattering, Fourier-Transformed Infrared spectroscopy (FTIR), Transmission Electron Microscopy (TEM), Photon Correlation Spectroscopy (PCS), Spontaneous Raman Scattering Spectroscopy and Multimodal Multiphoton Microscopy were used in the characterization and imaging of the polymer. See Supplementary Information for further details.

2.2. Preparation, characterization, dissolution and stability studies of AmB-GCPQ nanoparticles

Polyelectrolyte complex formation. AmB was solubilised through the formation of carboxylate salts at the concentration of 4 mg mL^{-1} in sodium hydroxide (0.02 N) at pH 12. GCPQ (20 mg mL^{-1}) was added to the solution. Polyelectrolyte complexes were formed between the carboxylic groups of the AmB and the positively charged quaternary ammonium groups of the GCPQ. The final pH of the dispersion was

reduced to pH = 5. AmB-GCPQ nanoparticles were centrifuged (13000 rpm, 30 min, Microcentaur, MSE, London, U.K.) to remove any aggregated polymer or undissolved drug and the supernatant was collected and characterised by PCS, FTIR and TEM. AmB aggregation state was assessed by UV.

Isocratic HPLC quantification of AmB. A validated analytical method utilising an Agilent 1200 series HPLC was used [17]. See Supplementary Information for method details.

Flow-through cell dissolution study (USP 4). A flow-through cell dissolution apparatus in an open-loop configuration and a cell of an internal diameter of 22.6 mm were used. Please see Supplementary Information Figure S1 for a schematic representation of the equipment used. The bottom cone of the cell was filled with one 5 mm diameter bead positioned at the apex, followed by 7 g of 1 mm diameter glass beads in order to generate a laminar flow. A NPcaps™ nº2 capsule (gelatin-like performance capsules made of Pullulan) filled with lyophilised formulation [either AmB-GCPQ or AmB deoxycholate (AMBd)] containing 5 mg of AmB was placed on the top of the small beads. A #40 mesh screen, a glass microfiber filter (Whatman® GF/D, 2.7 μm) and a 0.45 μm HA (mixed cellulose esters) hydrophilic filter (Millipore®) were positioned at the inner top of the cell to retain undissolved material. The dissolution medium was circulated by pumping it through the cell at a flow rate of 6 ml min^{-1}. Three dissolution media prepared as described in the US Pharmacopeia [18] were used during the experiment: simulated gastric fluid without enzymes (pH = 1.2) from 0 to15 min, acetate buffer (pH = 4.5) from 15 to 30 min and simulated intestinal fluid without enzymes (pH = 6.8) from 30 to 240 min. The temperature was maintained at 37 ± 0.5°C during testing. Samples were collected from the flow-through cell in fractions and scanned between 300 – 450 nm (Shimadzu UV-1700 spectrophotometer, Shimadzu,

Kyoto, Japan). Calibration curves were prepared using each of the dissolution media. The sum of the absorbance values at 406 and 328 nm (corresponding to the λ_{max} of the monomeric and dimeric AmB form respectively) was used to calculate the percentage of drug dissolved at each time point.

Long term stability studies. Stability studies were performed according to the International Conference on Harmonisation (ICH) guidelines Q1A (R2) [Stability testing of new drug substances and products] at 5°C ± 3°C for 12 months. NPcaps™ nº2 capsules were filled with 5 mg of lyophilised AmB-GCPQ formulation. Filled capsules were packaged in a blister made of poly(vinyl chloride) (PVC) with aluminium foil. At various time intervals, the contents of each capsule were dispersed in deionised water (at 1 mg mL^{-1}) and drug content and particle size were recorded (please see Supplementary Information for method details).

2.3. Pharmacokinetic studies in murine model

All experiments were performed under a UK Home Office Animal License.

Single dose oral administration of AmB formulations. CD-1 mice were randomly split into groups (n= 4), fasted overnight and then administered AmB formulations by oral gavage. Three different formulations of AmB were administered at an AmB dose of 5 mg kg^{-1} at the concentration of 1 mg mL^{-1}: (i) AmB-GCPQ (1: 5 g g^{-1}), (ii) AMBd (AmB, sodium deoxycholate, 1: 0.82 g g^{-1}, please see Supplementary Information for the preparation method) and (iii) AmB in 5% dextrose. Mice were sacrificed at different time points (0.5, 2, 4, 8, and 24 h) and blood and other organs (liver, spleen, brain, lungs, kidneys, bladder and gall bladder) were harvested. Plasma was separated by centrifugation (4500 rpm, 15 min, 4 °C, Hermle Z323K centrifuge, VWR, Poole, U.K.) and all tissues were stored at – 20 °C until analyses could be performed on them.

Multiple dose oral administration of AmB-GCPQ formulation. CD-1 mice were randomly divided into two groups (n = 3), fasted overnight and administered AmB by oral gavage. Oral gavages of AmB-GCPQ (1: 5 g g^{-1}) were administered at an AmB dose of 5 mg kg^{-1} and a concentration of 1 mg mL^{-1} for 5 days either twice daily (Group A) or once a day (Group B). Mice were sacrificed either 12 h (Group A) or 24 h (Group B) following the last administration of AmB-GCPQ. Blood and tissues (brain, liver, spleen, lungs, kidneys, bone marrow, bladder and gall bladder) were collected and stored as described above until samples could be analysed.

Intravenous (i.v.) administration of AmB-GCPQ formulation. Groups (n = 3) of male BALB/c mice were intravenously administered a freshly filtered (0.2 μm) AmB-GCPQ formulation (1: 5 g g^{-1}) at an AmB dose of 1 mg kg^{-1}. The formulation was previously diluted to 0.25 mg mL^{-1} with a solution of (1: 1) of sodium chloride (0.9% w/v) and dextrose (5% w/v). At various time intervals, animals were sacrificed (5 min, 30 min, 2 h, 4 h, 8 h, and 24 h) and blood was sampled. Plasma was separated and stored as described above.

AmB extraction. Plasma samples (100 μL) were spiked with the internal standard meloxicam (Fagrón SL., Madrid, Spain, 200 μg mL^{-1}, 10 μL) to a final concentration of 20 μg mL^{-1}. Extraction was carried out with methanol (300 μL). After vortexing, the mixture was centrifuged (10000 rpm, 10 min, Microcentaur, MSE, London, U.K.) and the supernatant evaporated to dryness under a stream of nitrogen. The samples were reconstituted in methanol (100 μL) and then centrifuged again (9000 rpm, 5 min, 4°C). The supernatants were analysed by the isocratic HPLC method previously described.

Tissue samples (liver, brain, kidneys, spleen, lungs and bone marrow) were added to sodium hydroxide solution (0.02 M) at pH 12 at a concentration of 0.5, 0.5, 0.25, 0.1, 0.1 and 0.1 g mL^{-1} tissue respectively homogenised. These tissue homogenates were

spiked with meloxicam (10 μg mL^{-1}, 400 μL) as described above. Two extractions of the aqueous tissue homogenate were carried out with methanol (2 mL x 2). After every extraction, the mixture was vortexed and then centrifuged (9000 rpm, 20 min, 4 °C). The supernatant (2 mL x 2) was collected and then evaporated to dryness under a stream of nitrogen. The samples were reconstituted with methanol, mobile phase (1: 1, 200 μL) consisting of acetonitrile, acetic acid, water (52: 4.3: 43.7, v/v/v)). After reconstitution, samples were centrifuged (13000 rpm, 5 min) and the supernatants analysed using a gradient HPLC method.

Urine was obtained after centrifuging bladder samples (13000 rpm, 5 min) Urine samples (10 μL) were spiked with meloxicam (200 μg mL^{-1}, 10 μL) and to this was added methanol (80 μL). Similarly, bile samples (the whole gallbladder) were spiked with meloxicam (200 μg mL^{-1}, 10 μL) and to this was added methanol (100 μL). After vortexing, samples were centrifuged (13000 rpm, 10 min) and the supernatants were analysed by a gradient HPLC method.

Gradient HPLC quantification of AmB. An HPLC gradient method utilising an Agilent 1200 series HPLC was developed to analyse the tissue samples. The samples (40 μL) were chromatographed over a Thermo Hypersil BDS C18 reverse-phase column (200 × 4.6 mm, 5 μm) maintained at 40°C, at a flow rate of 1.2 mL min^{-1}. The mobile phase consisted of 0.02 %w/v trifluoroacetic acid in water (line A) and acetonitrile (line B). The gradient method expressed as time (min): line B (%) was the following one: 0:10, 5:10, 15:59, 22:66, 28:90, 33:10. AmB and meloxicam were detected at a wavelength of 406 nm and their retention times were 16.0 and 16.6 min respectively. AmB concentrations were calculated from linear regression calibration curves from peak height ratios of AmB/ meloxicam.

2.4. Oral pharmacokinetic studies in beagles

All experiments were approved and performed in accordance with local ethics committee rules (University Cardenal Herrera-CEU, Valencia, Spain).

Animals. Healthy beagle dogs were housed according to the standards of the Committee of Animal Welfare, fed daily, and allowed free access to water throughout the study. Animal groups consisted of four male beagle dogs (weight = 15 - 19 kg) and one female beagle dog (weight = 15 kg), all of approximately 4 years of age.

Single dose oral administration of AmB formulations. Dogs were randomly assigned to receive orally either AmB-GCPQ formulation (n=3) or liposomal AmB (AmBisome®) (n=2) at 4 mg kg^{-1} of body weight. Prior to administration, AmBisome® was reconstituted with 5% w/v glucose at a final concentration of 4 mg mL^{-1}. AmB-GCPQ was prepared as previously described at a final AmB concentration of 4 mg mL^{-1}. After oral administration, blood sampling was carried out at time zero (predose), 15 min, 30 min, 60 min, 90 min, 2 h, 4 h, 6 h, 8 h, 24 h and 48 h. Plasma was separated by centrifugation and then stored at -20 ºC until analyses could be performed.

Extraction of AmB. Plasma samples (250 µL) were spiked with meloxicam (250 µg mL^{-1}, 10 µL) to a final concentration of 10 µg mL^{-1}. Two extractions were carried out with methanol (750 µL x 2), followed by a third extraction with acetonitrile (750 µL). After every extraction, the mixture was vortexed and centrifuged (9000 rpm, 10 min, 4°C). The supernatants were pooled (750 µL x 3) and, evaporated to dryness in a concentrator (Savant, SpeedVac®, Holbrook, NY, USA) at 30°C. Samples were reconstituted with a methanol, mobile phase solution (1:1, 250 µL). The mobile phase consisted of acetonitrile, acetic acid, water (52: 4.3: 43.7, v/v/v). The reconstituted

samples were centrifuged (9000 rpm, 5 min, 4°C) and the supernatants were analysed by the isocratic HPLC method previously described [17].

2.5. Efficacy study in a systemic murine model of visceral leishmaniasis

Animals. BALB/c mice (20-25 g) were randomly split into 5 groups (n = 8) and allowed food and water *ad libitum*. All experiments were approved by the Complutense University of Madrid Institutional Animal Care and Ethics Committee.

Infection. The preparation of the parasites and the experimental infection were performed as previously described [19]. Please see Supplementary Information for further details. Each animal was infected with 10^7 promastigotes by intracardiac injection.

Treatment. All treatments started on day 24 post-infection. Group A received intraperitoneal (i.p.) AmBisome® at a single dose of 5 mg kg^{-1}. Prior to administration, AmBisome® was reconstituted with water for injection to an AmB concentration of 4 mg mL^{-1} and then further diluted with glucose (5% w/v) to a final concentration of 1 mg mL^{-1}. Group B received an oral (p.o.) dose of the AmB-GCPQ formulation (AmB, GCPQ, 1: 5 g g^{-1}) at a dose of 5 mg kg^{-1} daily for five consecutive days. Group C served as an untreated control for groups A and B. Group D was treated orally with the same formulation as group B (AmB-GCPQ) at a dose of 5 mg kg^{-1} daily for ten consecutive days. Group E served as an untreated control for group D. Animals were sacrificed on day 31 (groups A, B and C) or day 36 (groups D and E) post- infection. Spleens and livers from each animal were aseptically removed and weighed to quantify the parasite burdens. Plasma and kidneys were collected to quantify the concentration of AmB. Plasma was separated by centrifugation and then both the plasma and kidneys were stored at -20 ºC until they could be analysed.

Tissue burden. The parasite burden was quantified by the limit dilution assay as described previously [20, 21]. Please see Supplementary Information for further details. The percentage suppression of parasite replication (PS) was calculated using the following modified equation of Manandhar et al.[22]:

PS = (PC-PT) / PC x 100 (Equation 1);

where PC is the number of parasites in the control group per tissue weight (g) and PT is the number of parasites after treatment per tissue weight (g).

Pharmacokinetic studies. Plasma and kidney samples were analysed as described above for the quantification of AmB in tissues.

2.6. Efficacy study in a systemic murine model of aspergillosis

Animals. Four week old OF-1 male mice (weight = 30 g) allowed food and water *ad libitum* were used. Animals were immunosuppressed one day before infection by a single i.p. dose of cyclophosphamide (200 mg kg^{-1}) and a single intravenous (i.v.) dose of fluorouracil (150 mg kg^{-1}). All experiments were approved by the Universitat Rovira i Virgili Institutional Animal Care and Ethics Committee.

Infection. One clinical isolate of *Aspergillus fumigatus* (FMR 7739) showing an AmB minimum inhibitory concentration of 1 µg ml^{-1} (determined by following Clinical and Laboratory Standards Institute guidelines) was used. The fungus was grown on potato dextrose agar (PDA) for 5 days at 35 ºC until sporulation occurred. The inoculum was prepared by flooding the plate surface with saline solution. The fungal suspension was filtered twice through sterile gauze to remove hyphae and clumps of agar and adjusted to the desired concentration by haemocytometer counting. To verify the viability and size of the inocula, 10 fold dilutions were placed in PDA for colony forming units

(CFU) determination. Animals were challenged i.v. via the lateral tail vein with a conidial suspension containing $1x10^4$ CFU in 0.2 ml of saline solution.

Treatment All treatments were started 24 h post infection and lasted for 10 days. Prior to administration, formulations were reconstituted with water for injection to an AmB concentration of 4 mg mL^{-1} and then further diluted with glucose (5% w/v) to a final concentration of 1 mg mL^{-1}. In the first experiment, groups of animals (n = 10) received AmBisome® administered i.v. at a dose of 5 mg kg^{-1} day^{-1}, AMBd administered i.v. at a dose of 0.8 mg kg^{-1} day^{-1}, AMBd administered p.o. at 5 mg kg^{-1} day^{-1} or AmB-GCPQ administered p.o. at 5 mg kg^{-1} day^{-1}. In the second experiment, groups of animals (n = 15) received AmBisome® administered i.v. at 2.5 mg kg^{-1} day^{-1}, AMBd administered i.v. at 0.5 mg kg^{-1} day^{-1}, AMBd administered p.o. at 2.5 mg kg^{-1} day^{-1} or AmB-GCPQ administered p.o. at 2.5 mg kg^{-1} day^{-1}. In the third experiment, groups of animals (n = 15) received AmBisome® administered i.v. at 5 mg kg^{-1} day^{-1}, AMBd administered i.v. at 0.8 mg kg^{-1} day^{-1}, AmB-GCPQ administered p.o. at 7.5 mg kg^{-1} day^{-1} or 15 mg kg^{-1} day^{-1}. One group without treatment was included as a control in all the experiments.

Tissue burden Eight days post infection, 5 animals from each group were sacrificed. Kidneys and lungs were removed, mechanically homogenized in 0.9% saline, diluted ten-fold in 0.9% saline and the homogenate placed on PDA plates for CFU g^{-1} determination.

2.7. Efficacy study in a systemic murine model of candidiasis

Animals. Male BALB/c mice were randomly split into 3 groups (n = 5) and allowed food and water *ad libitum*. All experiments were approved by the Complutense University of Madrid Institutional Animal Care and Ethics Committee.

Infection. One clinical isolate of *Candida albicans* CECT 1394 was used. Cultures were grown on Sabouraud dextrose agar for 48 h at 30 °C. A colony was resuspended in Yeast Extract Peptone Dextrose (YPD) broth (100 mL) and incubated at 30°C overnight. The log-phase *Candida* suspension was centrifuged (3000 rpm, 10 min, 4°C), washed two times with phosphate-buffered saline (PBS) and diluted to a final concentration of 20 x 10^6 CFU mL^{-1}. BALB/c mice were inoculated i.v. via the lateral tail vein with 1 x 10^6 CFU in PBS (50 µL).

Treatment. Treatment started 24 h following infection and lasted for 9 days. Prior to administration, formulations were reconstituted with water for injection to an AmB concentration of 4 mg mL^{-1} and then further diluted with glucose (5% w/v) to a final concentration of 1 mg mL^{-1}. Groups (n = 5) were treated either with AmB-GCPQ p.o. at 5 mg kg^{-1} day^{-1} or Ambisome® i.p. at 3 mg kg^{-1} day^{-1}. Another group of mice treated p.o. with deionized water: 5% glucose (1: 3) was included as a control.

Tissue burden. Mice were sacrificed by chloroform inhalation at day 10 post-infection and target organs (kidneys, liver, lung, brain and spleen) were removed aseptically, weighed, and homogenized in sterile saline (5 ml g^{-1} tissue). The number of CFU was determined by a plate dilution method in duplicate using yeast extract dextrose chloramphenicol agar and colony counting was performed after 72 h of incubation at 30 °C.

Toxicological and pharmacokinetic studies. Blood samples were collected at day 10 post-infection and serum was separated by centrifugation (3000 rpm, 10 min, 4°C). Samples were stored at −20°C for biochemistry analysis including creatinine, urea, alkaline phosphatase, aspartate transaminase (AST), alanine transaminase (ALT) and

bilirubin. Samples from healthy mice were included as controls. For pharmacokinetic studies, AmB concentrations in kidney, liver, brain and spleen were determined.

2.8. Statistical analysis

Statistical analyses were performed via one-way ANOVA Test using Minitab 15 (Minitab Ltd, Coventry, UK) followed by Tukey's test. Statistical significance was set at a $p < 0.05$.

3. Results

3.1. AmB-GCPQ interaction

GCPQ (Mw = 9,955 Da, Mn = 9,135 Da, Mw/Mn = 1.090, dn/dc = 0.1355 ± 0.0028 mL g^{-1}, 16.9 mole % palmitoylation and 16.5 mole % quaternary ammonium groups, HI = 1.02) was synthesised and characterised. The FTIR spectrum shows the interaction between AmB and GCPQ (Figure 1a) with an electrostatic complex being formed. This is evidenced by the fact that the signal from the carboxylate groups of the AmB at 1691 cm^{-1} (C=O stretch) disappears as does the C-N stretch signal from the GCPQ quaternary ammonium group (1246 cm^{-1}). The molar ratio of hydrophobic to hydrophilic groups (HI) in GCPQ plays a crucial role in its complexation with AmB. Polymers with higher palmitoylation (> 25%) or lower quaternization (< 15%) failed to form nanosized complexes and resulted in a liquid containing larger (> 1 μm) aggregates.

In aqueous environments, GCPQ self-assembles to form polymeric micelles with a particle size of between 5 – 30 nm in diameter while AmB itself aggregates forming insoluble polyhedral crystals (see Supplementary Information Figure S2). The AmB, GCPQ interaction resulted in the solubilisation of AmB crystals followed by the formation of highly stable nanoparticles characterised by a particle size of 216 and 35 nm (Figure 1b). The biomodal size is due to an equilibrium being established between drug filled particles and empty micelles. The particles have a core shell structure with the ionic units (and hence dark stained areas) forming the particle shells and the hydrophobic groups (white stain free areas) forming the particle core (Figure 1 b). The polar head of the AmB molecules will be oriented to the aqueous phase and the hydrophobic tail to the core of the nanoparticles. The hydrophobic tail of the polymer has the same number of carbons as the hydrophobic domain of AmB which should

enhance the hydrophobic interaction (see Supplementary Information Figure S2). The amount of amphotericin B loaded in nanoparticles was 90% as quantified in the supernatant obtained after centrifugation. Dimers and monomers of AmB were encapsulated in the polymer exhibiting characteristic absorption peaks at 328, 363, 383 and 407 nm and resulting in a transparent yellow liquid [7].

Lyophilised AmB-GCPQ nanoparticles exhibited good long term stability when stored at 5 ± 3 °C (particle size and drug content remained unaltered over one year, See Supplementary Information Figure S3) and these particles significantly enhanced AmB dissolution in simulated gastrointestinal fluids when compared to AMBd (Figure 1c).

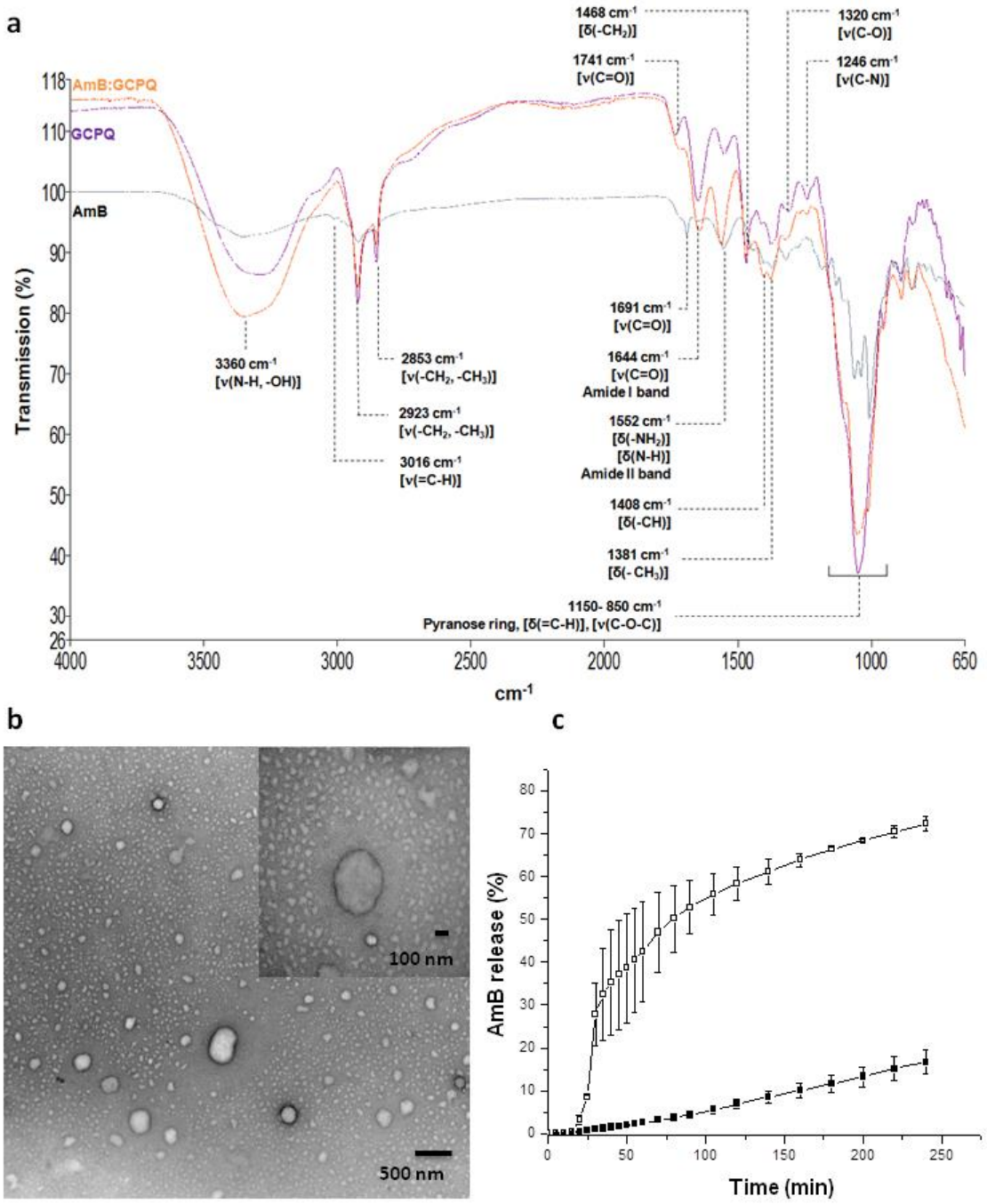

Figure 1. AmB-GCPQ interaction. (a) FTIR spectrum of AmB raw material, GCPQ and AmB-GCPQ nanoparticles after freeze drying. Key: ν - stretching vibrations; δ – bending vibrations. (b) TEM with negative staining of AmB (8 mg mL^{-1})-GCPQ (40 mg mL^{-1}) nanoparticles in deionized water. (c) Dissolution profile of AmB-GCPQ nanoparticles (-□-) versus AMBd (-■-).

3.2. Drug Pharmacokinetics

Mouse plasma and tissue concentration, time profiles of AmB following a single oral administration of AmB-GCPQ, AMBd or AmB in dextrose are shown in Figures 2a - e. Formulation characterisation data and pharmacokinetics parameters may be found in Supplementary Information Tables S1 and S2. With all formulations AmB plasma concentrations increased slowly and were sustained for 8 h after (Figure 2a). However the drug was largely tissue bound and accumulated in the liver, spleen and lung (Figure 2b, 2c, 2d). AmB-GCPQ resulted in higher plasma levels when compared to AmB in dextrose. Significantly higher AmB levels were found in the liver when the particulate formulations of AmB (AmB – GCPQ and AMBd) were administered compared to AmB in dextrose (Figure 2b). Significantly higher levels of AmB were found in the lungs and spleen, after oral administration of AmB-GCPQ compared to the administration of AmB in dextrose and AMBd. Only minor differences were found in AmB kidney levels, with respect to the formulation administered (Figure 2e). As AmB is a nephrotoxic drug, target organ, kidney ratios are crucial. Lung, kidney $AUC_{0\text{-}24}$ ratios for AmB-GCPQ and AMBd were 1.44 and 0.86 respectively while the corresponding spleen, kidney ratios were 1.22 and 0.81 respectively and the corresponding liver, kidney ratios were 0.88 and 0.40 respectively. These data demonstrate that, when compared to the deoxycholate micelles, GCPQ nanoparticles delivered relatively more drug to the target organs (liver, lung and spleen) than was delivered to the kidney. This finding is further confirmed by lower urine levels of AmB with the oral AmB-GCPQ formulation (Supplementary Information Figure S4a). The AmB in dextrose formulation delivered the most drug to the kidneys at the early time points, showing the drug in solution is rapidly eliminated by the kidneys; a fact that could contribute to the occurrence of nephrotoxicity and would explain the reduced drug levels in the target

organs with the AmB in dextrose formulation. AmB was also recovered from the gall bladder, reaching a maximum concentration at 4 hours following oral administration (see Supplementary Information Figure S4b). This is evidence of enterohepatic circulation of the drug. After 4 h, AmB levels in the bile decreased as a result of the animals being fed. The percentage of the AmB dose recovered from tissues (liver, spleen, lungs, kidneys) and plasma, 8 h after dosing the AmB-GCPQ formulation was 2.3%, which is 2-fold higher than when the drug was administered orally in dextrose.

After the administration of multiple doses of AmB-GCPQ to mice, AmB accumulated in the target organs (lungs, liver and spleen) and to a lesser extent in the kidney (Figure 2f and Supplementary Information Table S2). AmB-GCPQ also delivered AmB to the bone marrow and brain; the former important for the clearance of *Leishmania* and the latter important for the targeting of systemic fungal infections. AmB bile levels, following multiple doses, were significantly enhanced when compared to urine levels, further confirming a major role for enterohepatic circulation in AmB-GCPQ's delivery mechanism.

When a single dose of AmB-GCPQ was administered to dogs, again oral absorption was sustained for up to 8 h (Figure 2g). Plasma levels in dogs with oral AmB-GCPQ were over two fold higher than plasma levels seen with the oral administration of a nanoparticle formulation – AmBisome®. With AmB-GCPQ the plasma half-life ($t_{1/2}$) was 59.2 h in dogs and drug was still detectable in the plasma 48 h after dosing, whereas it was not detectable 48 h after dosing with oral AmBisome® in dogs. Both formulations were well tolerated and there were no signs of gastrointestinal toxicity (vomiting or diarrhoea).

After i.v. administration of AmB-GCPQ (Figure 2 h), there was a fast decline in the AmB plasma level, followed by a slower disappearance of the drug from the plasma

compartment as it equilibrates with the tissue bound drug. Similar high AmB tissue distributions have been observed by others [23, 24]. The absolute oral bioavailability of AmB-GCPQ was 24.7%. Similar oral bioavailability values have been reported for plain GCPQ nanoparticles[16]. The plasma $t_{1/2}$ of the AmB-GCPQ formulation in mice was 61.3 h.

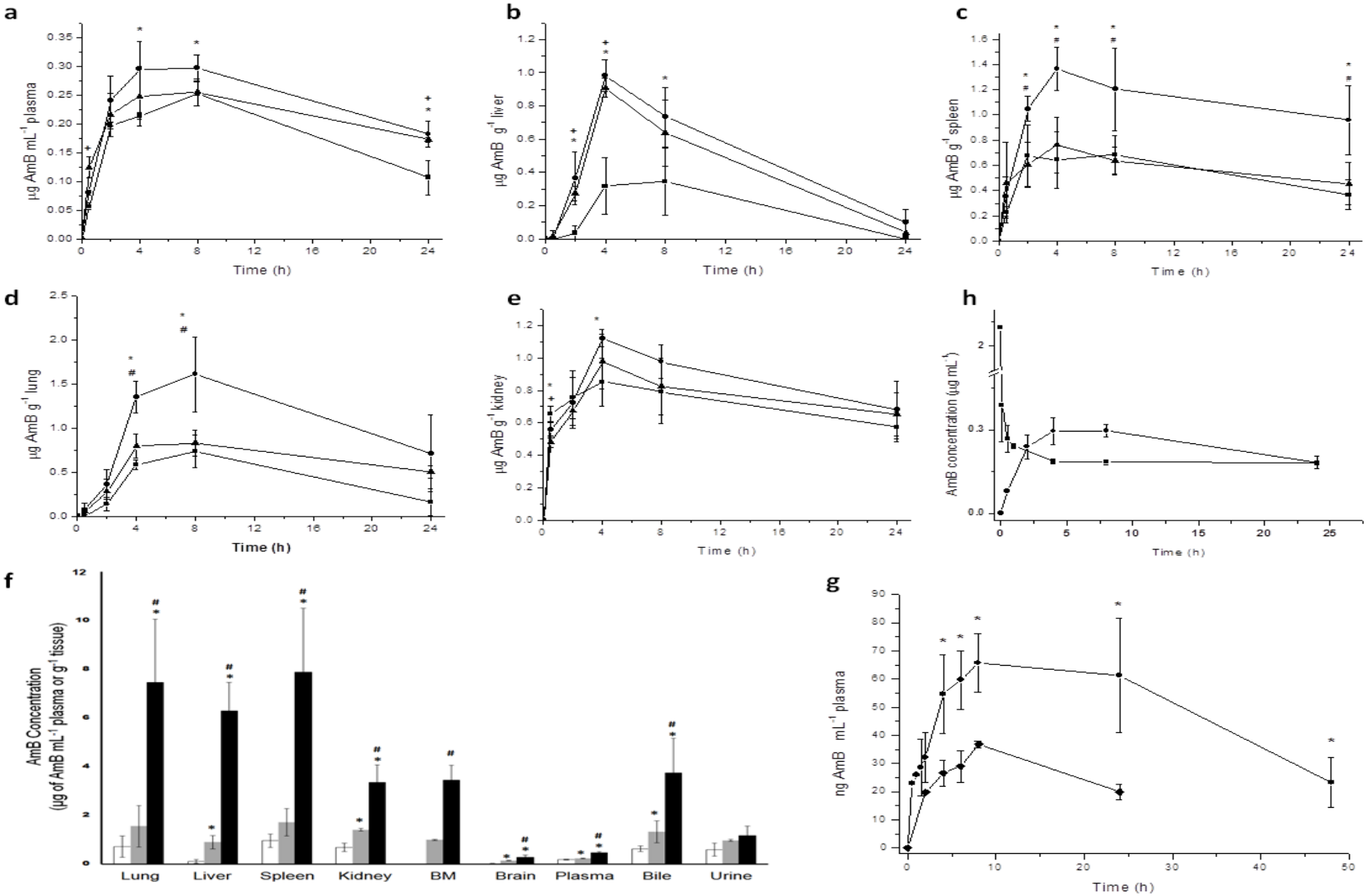
a
µg AmB mL-1 plasma
Time (h)
b
µg AmB g-1 liver
Time (h)
c
µg AmB g-1 spleen
Time (h)
d
µg AmB g-1 lung
Time (h)
e
µg AmB g-1 kidney
Time (h)
h
AmB concentration (µg mL-1)
Time (h)
f
AmB Concentration
(µg of AmB mL-1 plasma or g-1 tissue)
Lung
Liver
Spleen
Kidney
BM
Brain
Plasma
Bile
Urine
g
ng AmB mL-1 plasma
Time (h)

Figure 2. Pharmacokinetic studies: oral AmB translocation to major target organs. (a-e) Single dose oral administration of AmB formulations at 5 mg kg^{-1} in CD-1 mice. Key: AmB in dextrose (-■-); AMBd (-▲-); AmB (5 mg kg^{-1})- GCPQ (25 mg kg^{-1}) formulation (-●-). (a) AmB plasma levels (µg mL^{-1}). (b) AmB concentration in liver (µg g^{-1}). (c) AmB concentration in spleen (µg g^{-1}). (d) AmB concentration in lungs (µg g^{-1}). (e) AmB concentration in kidneys (µg g^{-1}). Statistical significant differences: * = $p < 0.05$ AmB-GCPQ versus AmB in dextrose; # = $p< 0.05$ AmB-GCPQ versus AMBd; + = $p< 0.05$ AmB in dextrose versus AMBd. **(f) Multiple dose oral administration of AmB-GCPQ**. AmB concentration in plasma and tissue distribution in major target organs after single and multiple dose administration in CD-1 mice. Key: AmB concentration at 24 hours after single oral administration of AmB-GCPQ formulation (at 5 mg kg^{-1}) (white); AmB concentration at 24 hours following the completion of once daily for 5 days oral treatment course of 5 mg kg^{-1} of AmB-GCPQ formulation (grey); AmB concentration at 12 hours following the completion of twice-daily for 5 days oral treatment course of 5 mg kg^{-1} of AmB-GCPQ (black). AmB levels in bone marrow (BM) after single oral administration were not quantified. Statistical significant differences: ***** = $p < 0.05$ versus oral single dose administration and # = $p< 0.05$ mutidose once-daily versus multidose twice-daily administration. **(g) AmB oral administration in beagles.** Key: AmB plasma concentration (mean ±SD) versus time profile after a single oral administration of AmBisome® (4 mg kg^{-1}) (-♦-) and AmB (4 mg kg^{-1})- GCPQ (20 mg kg^{-1}) nanoparticles (-■-) in beagles. AmB plasma concentration at 48 hours after orally administered AmBisome® was below the quantification limit of our method (15 ng mL^{-1}). Statistical significant differences: * = $p < 0.05$ AmB-GCPQ versus AmBisome®. **(h) AmB oral bioavailability**. AmB plasma concentration (mean ±SD) versus time profile after oral (-●-) and iv (-■-) administration of AmB-GCPQ formulation at the dose of 5 and 1 mg kg^{-1} respectively.

3.3. Oral Particle Translocation to Major Organs

The coherent anti-stokes Raman spectroscopy (CARS) method used, images highly concentrated species in a narrow focal area and only reports a signal for a self-assembled nanoparticle and not for individual polymer molecules as it is only with the former that the finite local concentrations are high enough to cross the resolution threshold for the technique. Using multimodal imaging techniques, deuterated GCPQ nanoparticles were imaged in the liver (Figure 3a), lungs (Figure 3b) and intestine (Figures 3c – e). Within the liver, GCPQ nanoparticles were located in the hepatocytes, the intercellular spaces between hepatocytes and bile canaliculi (Figure 3a); this is indicative of enterohepatic circulation and explains the prolonged oral absorption phase (Figure 2a). The presence of GCPQ particles in the liver (Figure 3a) and lung (Figure

3b) is explained by the fact that GCPQ particles are absorbed via the enterocytes as they were found within the intestinal villi (Figure 3c), from where they accessed the liver via the portal vein and systemic circulation and accessed the lung via the systemic circulation. GCPQ nanoparticles are not only taken up by the enterocytes but are also taken up by the Peyer's patches (Figure 3e) where they would have access to the systemic circulation via the lymphatic vessels. GCPQ nanoparticles are mucoadhesive [12] and they were found in the Brunner's glands of the duodenum (Figure 3d); the main function of the Brunner's glands is the secretion of a mucus-rich alkaline secretion into the duodenum. Please see Supplementary Information Figure S5 and Video 1 for additional details.

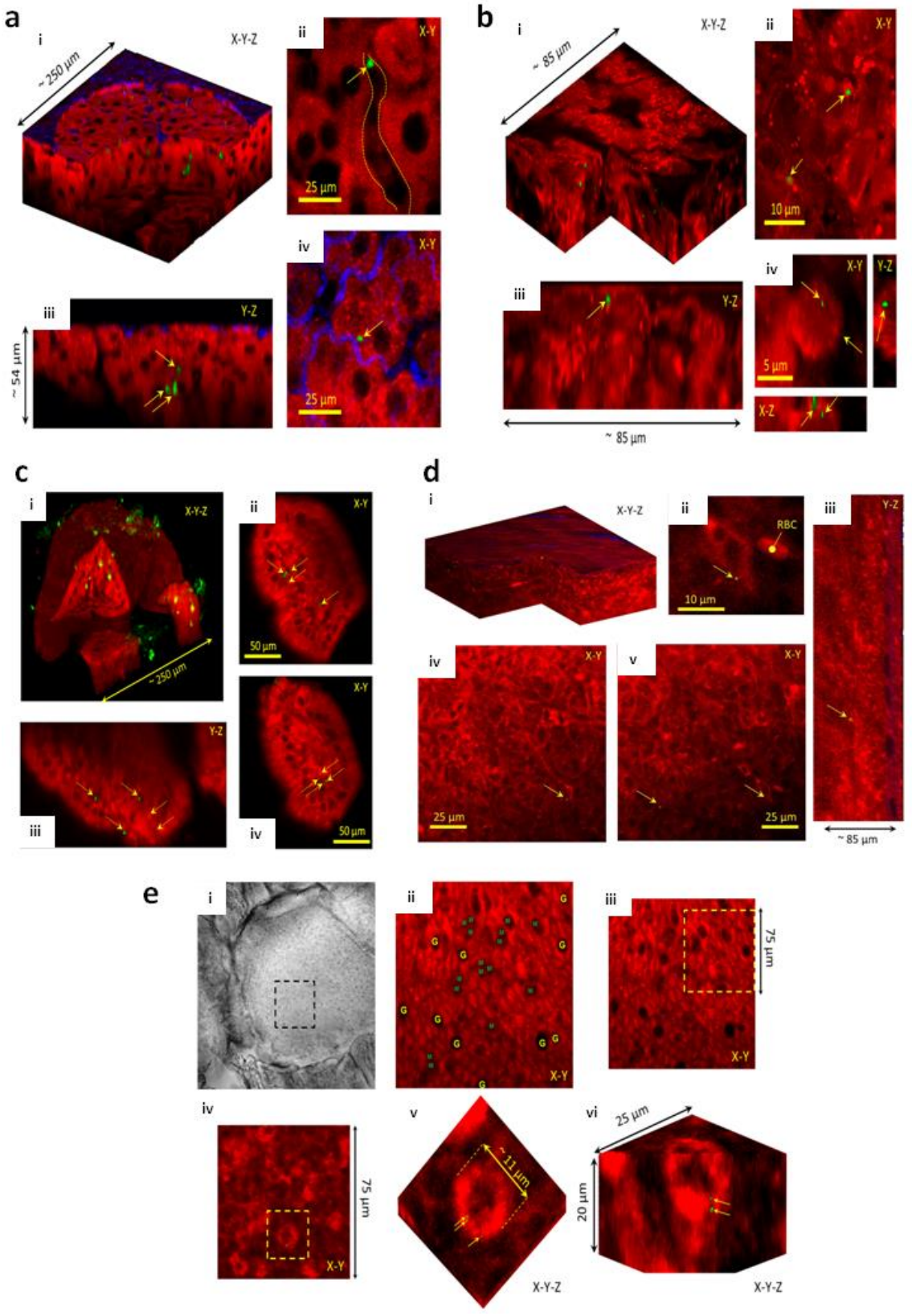

Figure 3. Multimodal multiphoton microscopy: oral AmB translocation to major target organs at 4 h after administration. (a) Liver. Three-dimensional multiphoton image reconstructions obtained from a liver sample. Two photon fluorescence (red) was used to generate contrast from endogenous fluorophores such as NADH, in addition to aldehyde-induced fluorescence from Schiff bases formed from the reaction of aldehydes

reacting with the tissue proteins' epsilon amino groups. Second harmonic generation provided contrast from collagen (blue). Contrast from deuterated particles was obtained with epi-detected CARS exciting the C-D resonance at 2100 cm^{-1} (green). The location of the deuterated particle signal is denoted by yellow arrows. **(b) Lungs.** Three-dimensional reconstructions of multiphoton images obtained from a lung sample. Red contrast was obtained from structures rich in C-H bonds, such as lipid droplets and cell membranes, using epi-detected CARS with the pump and Stokes beams tuned to excite the CH2 resonance (2845 cm^{-1}). Green contrast was obtained from deuterated particles with epi-detected CARS exciting the C-D resonance at 2100 cm^{-1}. **(c) Small intestine**. Three-dimensional reconstructions of multiphoton images obtained from a small intestine sample. Two photon fluorescence (red) – exciting contrast from endogenous fluorophores such as NADH, in addition to aldehyde-induced fluorescence from Schiff bases formed from the reaction of aldehydes reacting with the tissue proteins' epsilon amino groups. Green contrast was obtained from deuterated particles with epi-detected CARS exciting the C-D resonance at 2100 cm^{-1}. Within the villus cross sections, it is possible to see deuterated GCPQ has crossed the enterocyted (ii, iii and iv). Deuterated GCPQ signal is also found in association with mucus above the villi's surface in the three-dimensional reconstruction in (i). (**d) Brunner's gland**. Three-dimensional multiphoton image reconstruction of Brunner's glands. Red contrast was obtained from structures rich in C-H bonds, such as lipid droplets and cell membranes, using epi-detected CARS with the pump and Stokes beams tuned to excite the CH2 resonance (2845 cm^{-1}). Green contrast was obtained from deuterated particles with epi-detected CARS exciting the C-D resonance at 2100 cm^{-1}. Blue contrast arises from SHG of collagen within the sample. **(e) Peyer's patch.** i) Transmitted light image at low magnification, illustrating a Peyer's patch and surrounding villi. ii – vi) Epi-detected CARS image composites (red shows contrast from the CH stretch obtained with the pump and Stokes beams tuned to 2855 cm^{-1}, green shows contrast from the CD stretch obtained with the pump and Stokes beams tuned to 2100 cm^{-1}.) ii and iii were taken at the surface of the Peyer's patch, with M-cells and goblet cells marked with 'M' and 'G' respectively on B. iv was taken 14 microns below the surface, in the region outlined with a yellow box on iii. The cell outlined with a yellow box in iv is shown in more detail in v and vi, in three-dimensional composites of the CARS depth stack, illustrating the distribution of dGCPQ within this cell.

3.4. Efficacy in visceral leishmaniasis

The oral administration of AmB-GCPQ nanoparticles at 5 mg kg^{-1} day^{-1} for 10 days was similarly efficacious, in a murine model of visceral leishmaniasis, as a parenteral dose of AmBisome® (Figure 4). No statistical significant differences were observed between both therapies in the inhibition of parasite replication in liver (98.9% and 99.8%) and in spleen (92.1% and 95.2%) respectively. However, oral administration of AmB-GCPQ

for only 5 days was not sufficient to reduce parasite replication being less effective than parenterally administered AmBisome® (data no shown).

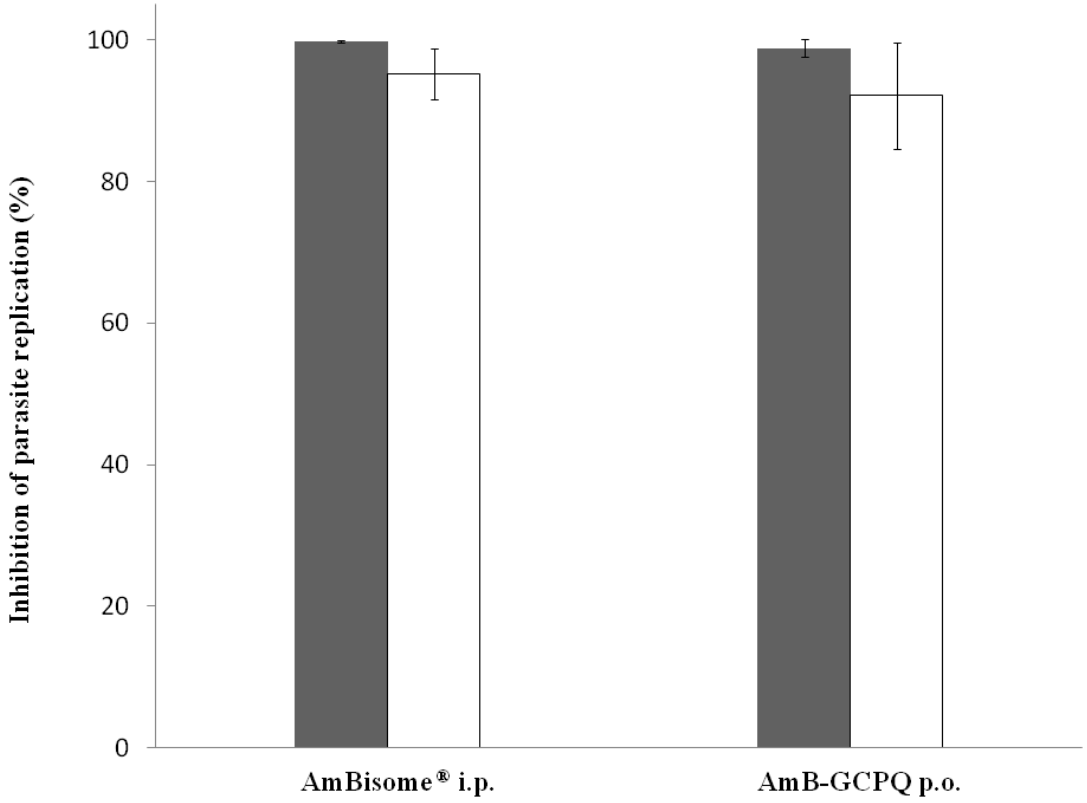

Figure 4. **Antileismanial activity of oral AmB-GCPQ nanoparticles in L. *infantum*-infected BALB/c mice**. All treatments started 24 days post-infection. Groups of animals (n = 8) received either AmBisome® i.p. at a single dose of 5 mg kg^{-1} body weight or orally AmB-GCPQ formulation at 5 mg kg^{-1} once-daily for 10 consecutive days. The parasitic burden was estimated by the limit dilution assay. Key: percentage of suppression of parasite replication in liver (grey) and spleen (white). Data are expressed as mean ± SD. Statistical significant differences ($p < 0.05$) were not found between both regimens.

AmB plasma levels 7 days after a single i.p. dose of Ambisome® (at 5 mg kg^{-1}), 3 days after the last oral dose of AmB-GCPQ 10 day course (at 5 mg kg^{-1} day^{-1} for 10 days) or 3 days after the last oral dose of AmB-GCPQ 5 day course (at 5 mg kg^{-1} day^{-1} for 5 days) were: 66.6 ± 22.9 ng mL^{-1}, 53.5 ± 15.9 ng mL^{-1} and 43.8 ± 20.9 ng mL^{-1} respectively; whereas the corresponding AmB kidney levels were: 1443.6 ± 662.4 ng g^{-1}, 578.9 ± 156.1 ng g^{-1} and 331.2 ± 101.1 ng g^{-1} respectively and plasma, kidney ratios

were: 0.046, 0.092 and 0.132 respectively showing increased distribution to the kidney with Ambisome®.

3.5. Efficacy in disseminated aspergillosis

A low oral AmB-GCPQ dose (2.5 mg kg^{-1} day^{-1}) did not increase the survival time or reduce the fungal burden in a murine model of disseminated aspergillosis (Figure 5a and 5b), whereas oral AmB-GCPQ was efficacious at higher doses. No significant difference in survival time, when compared to an untreated control group, was found between oral AmB-GCPQ (at 5 mg kg^{-1} day^{-1}) and i.v. Ambisome® (at 5 mg kg^{-1} day^{-1}) (Figure 5c). Intravenous AMBd (at 0.8 mg kg^{-1} day^{-1}) did not increase survival time compared to the control group (Figure 5c). In contrast to oral AMBd (at 0.8 mg kg^{-1} day^{-1}) oral AmB-GCPQ (at 5 mg kg^{-1} day^{-1}) reduced tissue burden with respect to controls (1.3 Log_{10} and 2.75 Log_{10} in kidney and lung respectively (Figure 5d). Higher oral AmB-GCPQ doses (at 7.5 or 15 mg kg^{-1} day^{-1}) were statistically similar to Ambisome® i.v. (at 5 mg kg^{-1} day^{-1}) (Figure 5e) and showed an even greater reduction in fungal load when compared to the lower dose of oral AmB-GCPQ (Figure 5f). No differences in efficacy were found between the 7.5 and 15 mg kg^{-1} day^{-1} oral doses of AmB-GCPQ (Figures 5e and 5f). Animals receiving oral AmB-GCPQ gained weight over time at all doses, whereas mice treated with oral AMBd suffered significant weight loss, presumably caused by the gastrointestinal toxicity of the formulation (see Supplementary Information Figure S6).

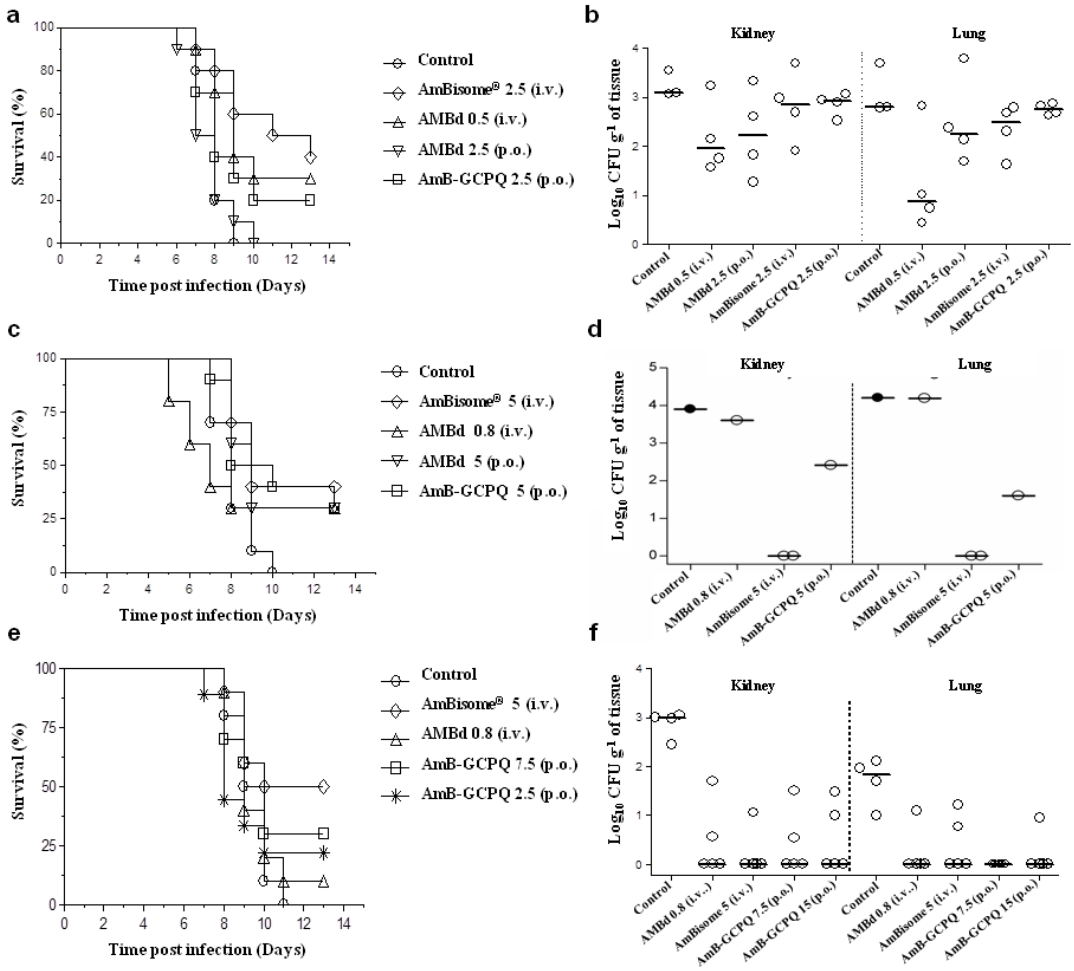

Figure 5. **Efficacy of AmB-GCPQ nanoparticles in a systemic murine model of aspergillosis.** On the left, survival of OF-1 mice infected intravenously (i.v.) with $1x10^4$ CFU of *A. fumigatus* after treatment is shown. On the right side, scattergram of CFU g^{-1} of tissue (kidney and lungs) is represented showing the median of the group by horizontal lines. Drugs were administered i.v. or orally by gavage (p.o.) 24h after infection for 10 days in the survival study or for 7 days in tissue burden study. **a-b)** Animals received liposomal AmB (AmBisome®) i.v. at 2.5 mg kg^{-1} day^{-1}, amphotericin B deoxycolate (AMBd) i.v. at 0.5 mg kg^{-1} day^{-1} and p.o. at 2.5 mg kg^{-1} day^{-1} or AmB-GCPQ nanoparticles p.o. at 2.5 mg kg^{-1} day^{-1}; **c-d)** Animals received AmBisome® i.v. at 5 mg kg^{-1} day^{-1}, AMBd i.v. at 0.8 mg kg^{-1} day^{-1} and p.o. at 5 mg kg^{-1} day^{-1} or AmB-GCPQ p.o. at 5 mg kg^{-1} day^{-1}; **e-f)** Animals received AmBisome® i.v. at 5 mg kg^{-1} day^{-1}, AMBd i.v. at 0.8 mg kg^{-1} day^{-1} or AmB-GCPQ p.o. at 7.5 and 15 mg kg^{-1} day^{-1}.

3.6. Efficacy in systemic candidiasis

Although AmB levels in tissues (kidney, liver, spleen and brain) after 9 days of parenteral Ambisome® (at 3 mg kg^{-1} day^{-1}) were significantly higher than those obtained after 9 days of oral AmB-GCPQ (at 5 mg kg^{-1} day^{-1}) (Figure 6b), no significant

differences were found in the reduction of fungal burden (Figure 6a and b) between both therapies. Oral AmB-GCPQ (at 5 mg kg^{-1} day^{-1}) cleared the spleen and liver and reduced by 1.4 log_{10} the fungal load in the brain compared to control animals.

The infected control group exhibited the highest levels of creatinine and urea as *C. albicans* infection is associated with renal failure[25] (Figure 6c and d). For example, mice with the highest CFU in kidney (mice 1, 2 and 4) exhibited the highest urea and creatinine levels. Oral administration of AmB-GCPQ resulted in a reduction of urea levels compared to the infected control group but produced a significant increase in alkaline phosphatase levels (Figures 6c and h). No significant differences were observed among the other biochemical parameters (Figures 6e -g).

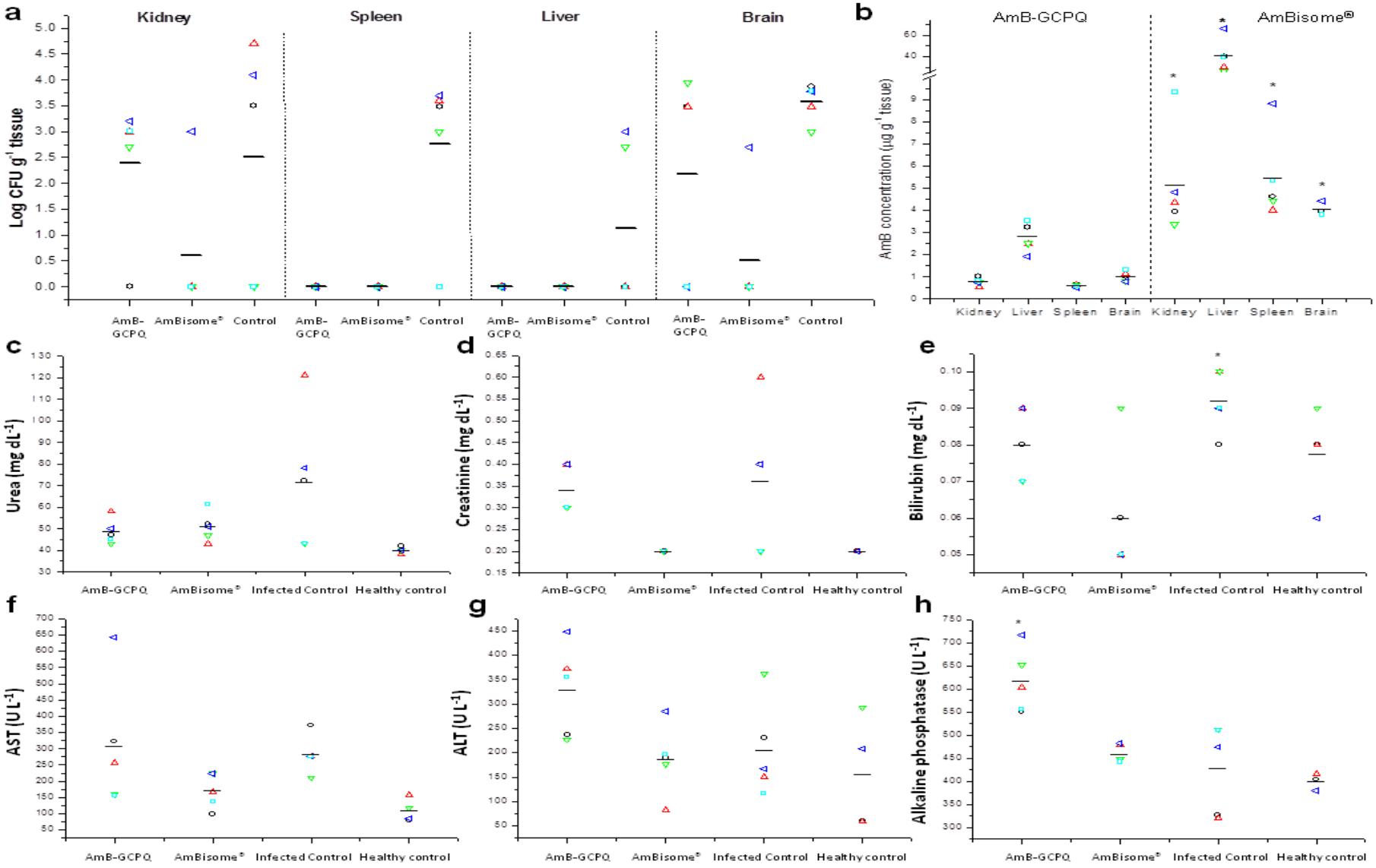
a
Kidney
Spleen
Liver
Brain
Log CFU g-1 tissue
AmB-GCPQ
AmBisome®
Control
b
AmB-GCPQ
AmBisome®
AmB concentration (µg g-1 tissue)
Kidney
Liver
Spleen
Brain
c
Urea (mg dL-1)
d
Creatinine (mg dL-1)
e
Bilirubin (mg dL-1)
f
AST (U L-1)
g
ALT (U L-1)
h
Alkaline phosphatase (U L-1)
AmB-GCPQ
AmBisome®
Infected Control
Healthy control

Figure 6. **PK/PD and toxicology correlation of AmB-GCPQ nanoparticles in a systemic murine model of candidiasis at day 10 post-infection.** Treatment started 24 h after infection and lasted for 9 days. Animals were treated with either liposomal AmB (AmBisome®) i.p. at 3 mg kg^{-1} day^{-1} or AmB-GCPQ p.o. at 5 mg kg^{-1} day^{-1}. One group was included as a control. A) Scattergram of CFU g^{-1} of tissue (kidney, spleen, liver and brain) is represented showing the median of the group by horizontal lines; b) AmB concentration (μg g^{-1}) in kidney, liver, spleen and brain. Statistical significant differences: * = $p < 0.05$ AmB-GCPQ versus AmBisome®; c) Urea levels (mg dL^{-1}); d) Creatinine levels (mg dL^{-1}); e) Bilirubin levels (mg dL^{-1}); statistical significant differences: * = $p < 0.05$ AmBisome® vs infected control group; f) AST (U L^{-1}); f) ALT (U L^{-1}); f) Alkaline phosphatase (U L^{-1}); statistical significant differences: * = $p < 0.05$ AmB-GCPQ vs all the groups. Key: mouse 1 (-○-); mouse 2 (-Δ-); mouse 3 (-▽-); mouse 4 (- ◁ -); mouse 5 (-□-); mean (▬).

4. Discussion

This is the first report in which orally administered nanoparticles (AmB-GCPQ) resulted in drug targeting to specific organs such as lung and spleen (Figures 2c, 2d and 3b). While both particle formulations (AmB-GCPQ and AMBd), deliver higher levels of drug to the liver (Figure 2b and Figure 3a), only the AmB-GCPQ formulation delivered drug specifically to the lung and spleen, while sparing of the organ of toxicity – the kidney (Figure 2e). This targeting to key organs (essentially to the lungs, liver and spleen) is of benefit to the treatment of a number of infectious diseases such as visceral leishmaniasis (Figure 4) and systemic fungal infections (Figures 5 and 6), with a drug such as AmB, which is a broad spectrum anti-fungal and low resistance anti-leishmanial drug but which is severely nephrotoxic. One aspect that contributes to the utility of the nanoparticles is the exceptional stability of the AmB-GCPQ nanoparticles. AmB-GCPQ nanoparticles are stable for one year on storage (Supplementary Information Figure S3). AmB-GCPQ nanoparticles are formed via electrostatic interactions between the AmB carboxylate and GCPQ quaternary ammonium groups (Figure 1a) as well as via the hydrophobic attractions between the palmitoyl chains of the GCPQ molecule and long chain alkene groups of the AmB molecule. The net result is a formulation of

exceptional stability, in which nanoparticles may be reconstituted from a dry powder (Supplementary Information Figure S3c).

AmB-GCPQ nanoparticles enhanced the oral absorption of AmB when compared to the drug alone or to the reference particulate formulation AMBd. AmB is poorly soluble in aqueous media (< 1 mg L^{-1})[7] and its poor dissolution rate within the gastrointestinal tract will limit absorption as will its poor gut permeation, since AmB is a Biopharmaceutical Classification System Class IV drug with poor gut permeability as well as poor aqueous solubility[26]. AMBd formulations will provide an increase in dissolution rate as AmB is encapsulated within small, high surface area deoxycholate micelles, however AmB-GCPQ nanoparticles will not only increase drug dissolution but will also be taken up via the gut enterocytes and Peyer's patches (Figures 3c and e) thus solving the gut permeation problems associated with AmB. GCPQ nanoparticles are positively charged and are known to be mucoadhesive[12], and taken up by the gut enterocytes with a bioavailability of 24%[13, 16] and now we also know that they are taken up by the Peyer's patches (Figure 3e). Transport from the gut associated lymphoid tissue via the lymphatic vessels to the systemic circulation will also increase the oral bioavailability of the AmB-GCPQ formulation.

In comparison to other oral AmB lipid-based formulations that have been reported [27-29], AmB-GCPQ nanoparticles are able to deliver greater amounts of drug to tissues after administering the same oral dose (5 mg kg^{-1} twice daily for 5 days); drug levels are 6.6 - 7.5 fold higher in liver, 8.6 - 10.5 fold greater in spleen, 5.2 – 6.4 fold higher in lungs and 2.5 fold higher in brain when compared to these other AmB lipid-based formulations. Furthermore this is the first study that reports an oral AmB relative bioavailability of 24.7%. High levels of AmB are found in the organs of the reticuloendothelial system (liver, lung, spleen and bone marrow) after oral absorption of

AmB-GCPQ (Figures 2 c – f) and this may be the result of macrophage phagocytosis of particles within the lymphatic vessels and systemic circulation. GCPQ nanoparticles on intravenous administration are not taken up by the spleen and only very low levels (4% of the administered dose at the 5 minute time point)[14] are found in the liver, whereas via the oral route GCPQ nanoparticles distribute to the spleen, liver and lung with 0.25, 2, 0.2% of a 200 mg kg-1 dose distributing to the spleen liver and lung at the 2h time point respectively [13, 16]. The AmB coating on the surface of the GCPQ nanoparticles (Figure 1b) would also contribute to uptake by macrophages as AmB is known to be cleared by the macrophages [7].

The treatment of infectious diseases requires sufficient drug levels in key organs and although, much lower AmB concentration were recorded in target organs after oral administration of AmB-GCPQ nanoparticles compared to after the parenteral administration of AmBisome®, there were no real differences in the efficacy of oral AmB-GCPQ, when compared to i.v. AmBisome® (Figures 4 – 6) with respect to the liver, spleen and lung microorganisms. However the lower levels of AmB found in the kidney on the oral administration of AmB-GCPQ did result in a poorer control of candidiasis fungal load in the kidney with this formulation (Figure 6a). This also explains the slow recovery of kidney function (creatinine levels, Figure 6d) on oral administration of AmB-GCPQ. While there were unexplained changes to the alkaline phosphatase levels after oral administration of AmB-GCPQ there were no significant differences in the other biochemical markers when AmB-GCPQ animals was compared to healthy controls.

This is also the first report on the oral absorption of AmB in dogs. Absorption of AmB from AmB-GCPQ is superior to that seen with an oral formulation of AmBisome® (Figure 2g). AmB-GCPQ is thus superior to other nanoparticle formulations such as

AMBd and AmBisome® in rodents and dogs respectively. Interspecies differences were noted in the oral AmB-GCPQ plasma level time curve data. The Cmax was lower in dogs when compared to mice (Figures 2a and 2g) and this could stem from differences in stomach pH (fasted dog stomach pH = 2.03 ± 0.59 [30] and fasted mouse stomach pH = 4.04 ± 0.2) [31] which would lead to a faster drug degradation in the dog or differences in bile flow (dog bile flow = 12 mL day^{-1} kg^{-1} [32] and mouse bile flow = 100 mL day^{-1} kg^{-1} [32]) which would lead to reduced hydrophobic drug absorption. Plasma levels dropped more steeply in the mouse compared to the dog during the elimination phase (8 – 24 h after dosing), with a drop of 38.8% in mice and 6.7% in dogs, and this could be due to the faster glomerular filtration rate in dogs (glomerular filtration rate = 14 and 6 mL min^{-1} kg^{-1} in mice and dogs respectively [32]).

So far, marketed AmB formulations have to be parenterally administered although in developing countries, there are neither enough technical personal nor clinical facilities to allow safe parenteral i.v. administration. In such countries oral drug administration should clearly be the first choice format. In this work, we have demonstrated that AmB accumulation in specific target organs may be achieved by the oral administration by AmB-GCPQ nanoparticles, resulting in high enough concentrations to elicit AmB's pharmacological effect, while sparing the site of drug toxicity – the kidney.

5. Conclusions

In summary, our work demonstrates, for the first time, that oral particle uptake and translocation to specific organs may be used to achieve a beneficial therapeutic response. We have designed an orally active nanomedicine based on an amphiphilic nanoparticle forming polymer (GCPQ), which achieves a relative AmB oral bioavailability of 24.7%. AmB-GCPQ nanoparticles target AmB to particular organs of

pathology and spare the site of toxicity – the kidney, resulting in effective treatments in preclinical disease models. This is the first report of a therapeutic advantage stemming directly from particle gut uptake and translocation to key organs of pathology. AmB liver, spleen and lung levels after oral AmB-GCPQ administration were lower than those obtained with parenteral formulations, however oral AmB-GCPQ was as effective as the parenteral AmBisome® formulation in the treatment of visceral leishmaniasis, aspergillosis and systemic candidiasis animal models of these diseases.

Supporting Information

This material is available free of charge via the Internet at http://pubs.acs.org.

Acknowledgements

David McCarthy (UCL School of Pharmacy) is acknowledged for providing transmission electron microscopy expertise. This work was financial supported by the UCL School of Pharmacy, Complutense University and Madrid Community Administration (research group 910939). D.R. Serrano is supported by a Research Fellowship FPU grant (AP2008-00235) from the Spanish Ministry of Education. J.G. and J.C. have received financial support from the EU 7th FP, grant 601963.

References

1. Kirkpatrick, P. Pressures in the pipeline. *Nature Reviews Drug Discovery* **2003,** *2*, 337.
2. Kola, I.; Landis, J. Can the pharmaceutical industry reduce attrition rates? *Nat Rev Drug Discov* **2004,** *3*, (8), 711-5.
3. Strickley, R. G. Solubilizing excipients in oral and injectable formulations. *Pharm. Res.* **2004,** *21*, (2), 201-230.
4. Jibodh, R. A.; Lagas, J. S.; Nuijen, B.; Beijnen, J. H.; Schellens, J. H. M. Taxanes: Old drugs, new oral formulations. *Eur. J. Pharmacol.* **2013,** *717*, (1-3), 40-46.

5. Chaturvedi, K.; Ganguly, K.; Nadagouda, M. N.; Aminabhavi, T. M. Polymeric hydrogels for oral insulin delivery. *J. Control. Rel.* **2013,** *165*, (2), 129-138.
6. Meyer, R. D. Current role of therapy with amphotericin B. *Clin Infect Dis* **1992,** *14 Suppl 1*, S154-60.
7. Torrado, J. J.; Espada, R.; Ballesteros, M. P.; Torrado-Santiago, S. Amphotericin B formulations and drug targeting. *J Pharm Sci* **2008,** *97*, (7), 2405-25.
8. Bes, D. F.; Sberna, N.; Rosanova, M. T. [Advantages and drawbacks of amphotericin formulations in children: literature review]. *Arch Argent Pediatr* **2012,** *110*, (1), 46-51.
9. Torrado, J.; Serrano, D.; Uchegbu, I. The oral delivery of amphotericin B. *Therapeutic Delivery* **2013,** *4*, (1), 9-12.
10. Ching, M. S.; Raymony, K.; Bury, R. W.; Mashford, M. L.; Morgan, D. J. Absorption of orally adminsitered amphotericin B lozenges *Br J Clin Pharmac* **1983,** *16*, 106-108.
11. Qu, X.; Khutoryanskiy, V. V.; Stewart, A.; Rahman, S.; Papahadjopoulos-Sternberg, B.; Dufes, C.; McCarthy, D.; Wilson, C. G.; Lyons, R.; Carter, K. C.; Schatzlein, A.; Uchegbu, I. F. Carbohydrate-based micelle clusters which enhance hydrophobic drug bioavailability by up to 1 order of magnitude. *Biomacromolecules* **2006,** *7*, (12), 3452-9.
12. Siew, A.; Le, H.; Thiovolet, M.; Gellert, P.; Schatzlein, A.; Uchegbu, I. Enhanced oral absorption of hydrophobic and hydrophilic drugs using quaternary ammonium palmitoyl glycol chitosan nanoparticles. *Mol Pharm* **2012,** *9*, (1), 14-28.
13. Garrett, N. L.; Lalatsa, A.; Uchegbu, I.; Schatzlein, A.; Moger, J. Exploring uptake mechanisms of oral nanomedicines using multimodal nonlinear optical microscopy. *J Biophotonics* **2012,** *5*, (5-6), 458-68.
14. Lalatsa, A.; Lee, V.; Malkinson, J. P.; Zloh, M.; Schatzlein, A. G.; Uchegbu, I. F. A prodrug nanoparticle approach for the oral delivery of a hydrophilic peptide, leucine(5)-enkephalin, to the brain. *Mol Pharm* **2012,** *9*, (6), 1665-80.
15. Uchegbu, I. F.; Sadiq, L.; Arastoo, M.; Gray, A. I.; Wang, W.; Waigh, R. D.; Schatzlein, A. G. Quaternary ammonium palmitoyl glycol chitosan--a new polysoap for drug delivery. *Int J Pharm* **2001,** *224*, (1-2), 185-99.
16. Lalatsa, A.; Garrett, N. L.; Ferrarelli, T.; Moger, J.; Schatzlein, A. G.; Uchegbu, I. F. Delivery of peptides to the blood and brain after oral uptake of quaternary ammonium palmitoyl glycol chitosan nanoparticles. *Mol Pharm* **2012,** *9*, (6), 1764-74.
17. Espada, R.; Josa, J. M.; Valdespina, S.; Dea, M. A.; Ballesteros, M. P.; Alunda, J. M.; Torrado, J. J. HPLC assay for determination of amphotericin B in biological samples. *Biomedical chromatography : BMC* **2008,** *22*, (4), 402-7.
18. The United States Pharmacopeial Convention Inc, The United States Pharmacopeia and National Formulary USP 32–NF 27. Rockville, MD, 2009.
19. Dea-Ayuela, M. A.; Castillo, E.; Gonzalez-Alvarez, M.; Vega, C.; Rolon, M.; Bolas-Fernandez, F.; Borras, J.; Gonzalez-Rosende, M. E. In vivo and in vitro anti-leishmanial activities of 4-nitro-N-pyrimidin- and N-pyrazin-2-ylbenzenesulfonamides, and N2-(4-nitrophenyl)-N1-propylglycinamide. *Bioorg Med Chem* **2009,** *17*, (21), 7449-56.
20. Hill, J. O.; North, R. J.; Collins, F. M. Advantages of measuring changes in the number of viable parasites in murine models of experimental cutaneous leishmaniasis. *Infect Immun* **1983,** *39*, (3), 1087-94.
21. Titus, R. G.; Marchand, M.; Boon, T.; Louis, J. A. A limiting dilution assay for quantifying Leishmania major in tissues of infected mice. *Parasite Immunol* **1985,** *7*, (5), 545-55.
22. Manandhar, K. D.; Yadav, T. P.; Prajapati, V. K.; Kumar, S.; Rai, M.; Dube, A.; Srivastava, O. N.; Sundar, S. Antileishmanial activity of nano-amphotericin B deoxycholate. *J Antimicrob Chemother* **2008,** *62*, (2), 376-80.
23. Bellmann, R. Clinical pharmacokinetics of systemically administered antimycotics. *Curr Clin Pharmacol* **2007,** *2*, 37-58.

24. Fielding, R. M.; Singer, A. W.; Wang, L. H.; Babbar, S.; Guo, L. S. Relationship of pharmacokinetics and drug distribution in tissue to increased safety of amphotericin B colloidal dispersion in dogs. *Antimicrob Agents Ch* **1992,** *36*, 299-307.
25. Nishimoto, G.; Tsunoda, Y.; Nagata, M.; Yamaguchi, Y.; Yoshioka, T.; Ito, K. Acute renal failure associated with Candida albicans infection. *Pediatr Nephrol* **1995,** *9*, (4), 480-2.
26. Wu, C. Y.; Benet, L. Z. Predicting drug disposition via application of BCS: transport/absorption/ elimination interplay and development of a biopharmaceutics drug disposition classification system. *Pharm. Res.* **2005,** *22*, (1), 11-23.
27. Sivak, O.; Gershkovich, P.; Lin, M.; Wasan, E. K.; Zhao, J.; Owen, D.; Clement, J. G.; Wasan, K. M. Tropically stable novel oral lipid formulation of amphotericin B (iCo-010): biodistribution and toxicity in a mouse model. *Lipids Health Dis* **2011,** *10*, 135.
28. Gershkovich, P.; Sivak, O.; Wasan, E. K.; Magil, A. B.; Owen, D.; Clement, J. G.; Wasan, K. M. Biodistribution and tissue toxicity of amphotericin B in mice following multiple dose administration of a novel oral lipid-based formulation (iCo-009). *J Antimicrob Chemother* **2010,** *65*, (12), 2610-3.
29. Risovic, V.; Boyd, M.; Choo, E.; Wasan, K. M. Effects of lipid-based oral formulations on plasma and tissue amphotericin B concentrations and renal toxicity in male rats. *Antimicrob. Agents Chemother.* **2003,** *47*, (10), 3339-42.
30. Sagawa, K.; Li, F.; Liese, R.; Sutton, S. Fed and Fasted Gastric pH and Gastric Residence Time in Conscious Beagle Dogs. *J. Pharm. Sci.* **2009,** *98*, (7), 2494-2500.
31. McConnell, E. L.; Basit, A. W.; Murdan, S. Measurements of rat and mouse gastrointestinal pH, fluid and lymphoid tissue, and implications for in-vivo experiments. *The Journal of pharmacy and pharmacology* **2008,** *60*, (1), 63-70.
32. Davies, B.; Morris, T. Physiological parameters in laboratory animals and humans. *Pharmaceutical research* **1993,** *10*, (7), 1093-5.

Figure captions

Figure 1. AmB-GCPQ interaction. (a) FTIR spectrum of AmB raw material, GCPQ and AmB-GCPQ nanoparticles after freeze drying. Key: ν - stretching vibrations; δ – bending vibrations. (b) TEM with negative staining of AmB (8 mg mL^{-1})-GCPQ (40 mg mL^{-1}) nanoparticles in deionized water. (c) Dissolution profile of AmB-GCPQ nanoparticles (-□-) versus AMBd (-■-).

Figure 2. Pharmacokinetic studies: oral AmB translocation to major target organs. (a-e) Single dose oral administration of AmB formulations at 5 mg kg^{-1} in CD-1 mice. Key: AmB in dextrose (-■-); AMBd (-▲-); AmB (5 mg kg^{-1})- GCPQ (25 mg kg^{-1}) formulation (-●-). (a) AmB plasma levels (μg mL^{-1}). (b) AmB concentration in liver (μg g^{-1}). (c) AmB concentration in spleen (μg g^{-1}). (d) AmB concentration in lungs (μg g^{-1}). (e) AmB concentration in kidneys (μg g^{-1}). Statistical significant differences: * = $p < 0.05$ AmB-GCPQ versus AmB in dextrose; # = $p< 0.05$ AmB-GCPQ versus AMBd; + = $p< 0.05$ AmB in dextrose versus AMBd. **(f) Multiple dose oral administration of AmB-GCPQ**. AmB concentration in plasma and tissue distribution in major target organs after single and multiple dose administration in CD-1 mice. Key: AmB concentration at 24 hours after single oral administration of AmB-GCPQ formulation (at 5 mg kg^{-1}) (white); AmB concentration at 24 hours following the completion of once daily for 5 days oral treatment course of 5 mg kg^{-1} of AmB-GCPQ formulation (grey); AmB concentration at 12 hours following the completion of twice-daily for 5 days oral treatment course of 5 mg kg^{-1} of AmB-GCPQ (black). AmB levels in bone marrow (BM) after single oral administration were not quantified. Statistical significant

differences: ***** = $p < 0.05$ versus oral single dose administration and **#** = $p < 0.05$ mutidose once-daily versus multidose twice-daily administration. **(g) AmB oral administration in beagles.** Key: AmB plasma concentration (mean ±SD) versus time profile after a single oral administration of AmBisome® (4 mg kg^{-1}) (-♦-) and AmB (4 mg kg^{-1})- GCPQ (20 mg kg^{-1}) nanoparticles (-■-) in beagles. AmB plasma concentration at 48 hours after orally administered AmBisome® was below the quantification limit of our method (15 ng mL^{-1}). Statistical significant differences: * = $p < 0.05$ AmB-GCPQ versus AmBisome®. **(h) AmB oral bioavailability**. AmB plasma concentration (mean ±SD) versus time profile after oral (-●-) and iv (-■-) administration of AmB-GCPQ formulation at the dose of 5 and 1 mg kg^{-1} respectively.

Figure 3. Multimodal multiphoton microscopy: oral AmB translocation to major target organs. (a) Liver. Three-dimensional multiphoton image reconstructions obtained from a liver sample. Two photon fluorescence (red) was used to generate contrast from endogenous fluorophores such as NADH, in addition to aldehyde-induced fluorescence from Schiff bases formed from the reaction of aldehydes reacting with the tissue proteins' epsilon amino groups. Second harmonic generation provided contrast from collagen (blue). Contrast from deuterated particles was obtained with epi-detected CARS exciting the C-D resonance at 2100 cm^{-1} (green). The location of the deuterated particle signal is denoted by yellow arrows. **(b) Lungs.** Three-dimensional reconstructions of multiphoton images obtained from a lung sample. Red contrast was obtained from structures rich in C-H bonds, such as lipid droplets and cell membranes, using epi-detected CARS with the pump and Stokes beams tuned to excite the CH2 resonance (2845 cm^{-1}). Green contrast was obtained from deuterated particles with epi-detected CARS exciting the C-D resonance at 2100 cm^{-1}. **(c) Small intestine**. Three-dimensional reconstructions of multiphoton images obtained from a small intestine

sample. Two photon fluorescence (red) – exciting contrast from endogenous fluorophores such as NADH, in addition to aldehyde-induced fluorescence from Schiff bases formed from the reaction of aldehydes reacting with the tissue proteins' epsilon amino groups. Green contrast was obtained from deuterated particles with epi-detected CARS exciting the C-D resonance at 2100 cm^{-1}. Within the villus cross sections, it is possible to see deuterated GCPQ has crossed the enterocyted (ii, iii and iv). Deuterated GCPQ signal is also found in association with mucus above the villi's surface in the three-dimensional reconstruction in (i). (**d) Brunner's gland**. Three-dimensional multiphoton image reconstruction of Brunner's glands. Red contrast was obtained from structures rich in C-H bonds, such as lipid droplets and cell membranes, using epi-detected CARS with the pump and Stokes beams tuned to excite the CH2 resonance (2845 cm^{-1}). Green contrast was obtained from deuterated particles with epi-detected CARS exciting the C-D resonance at 2100 cm^{-1}. Blue contrast arises from SHG of collagen within the sample. **(e) Peyer's patch.** i) Transmitted light image at low magnification, illustrating a Peyer's patch and surrounding villi. ii – vi) Epi-detected CARS image composites (red shows contrast from the CH stretch obtained with the pump and Stokes beams tuned to 2855 cm^{-1}, green shows contrast from the CD stretch obtained with the pump and Stokes beams tuned to 2100 cm^{-1}.) ii and iii were taken at the surface of the Peyer's patch, with M-cells and goblet cells marked with 'M' and 'G' respectively on B. iv was taken 14 microns below the surface, in the region outlined with a yellow box on iii. The cell outlined with a yellow box in iv is shown in more detail in v and vi, in three-dimensional composites of the CARS depth stack, illustrating the distribution of dGCPQ within this cell.

Figure 4. **Antileismanial activity of oral AmB-GCPQ nanoparticles in L. *infantum*-infected BALB/c mice**. All treatments started 24 days post-infection. Groups of

animals (n = 8) received either AmBisome® i.p. at a single dose of 5 mg kg^{-1} body weight or orally AmB-GCPQ formulation at 5 mg kg^{-1} once-daily for 10 consecutive days. The parasitic burden was estimated by the limit dilution assay. Key: percentage of suppression of parasite replication in liver (grey) and spleen (white). Data are expressed as mean ± SD. Statistical significant differences ($p < 0.05$) were not found between both regimens.

Figure 5. **Efficacy of AmB-GCPQ nanoparticles in a systemic murine model of aspergillosis.** On the left, survival of OF-1 mice infected intravenously (i.v.) with $1x10^4$ CFU of *A. fumigatus* after treatment is shown. On the right side, scattergram of CFU g^{-1} of tissue (kidney and lungs) is represented showing the median of the group by horizontal lines. Drugs were administered i.v. or orally by gavage (p.o.) 24h after infection for 10 days in the survival study or for 7 days in tissue burden study. **a-b)** Animals received liposomal AmB (AmBisome®) i.v. at 2.5 mg kg^{-1} day^{-1}, amphotericin B deoxycolate (AMBd) i.v. at 0.5 mg kg^{-1} day^{-1} and p.o. at 2.5 mg kg^{-1} day^{-1} or AmB-GCPQ nanoparticles p.o. at 2.5 mg kg^{-1} day^{-1}; **c-d)** Animals received AmBisome® i.v. at 5 mg kg^{-1} day^{-1}, AMBd i.v. at 0.8 mg kg^{-1} day^{-1} and p.o. at 5 mg kg^{-1} day^{-1} or AmB-GCPQ p.o. at 5 mg kg^{-1} day^{-1}; **e-f)** Animals received AmBisome® i.v. at 5 mg kg^{-1} day^{-1}, AMBd i.v. at 0.8 mg kg^{-1} day^{-1} or AmB-GCPQ p.o. at 7.5 and 15 mg kg^{-1} day^{-1}.

Figure 6. **PK/PD and toxicology correlation of AmB-GCPQ nanoparticles in a systemic murine model of candidiasis at day 10 post-infection.** Treatment started 24 h after infection and lasted for 9 days. Animals were treated with either liposomal AmB (AmBisome®) i.p. at 3 mg kg^{-1} day^{-1} or AmB-GCPQ p.o. at 5 mg kg^{-1} day^{-1}. One group was included as a control. A) Scattergram of CFU g^{-1} of tissue (kidney, spleen, liver and brain) is represented showing the median of the group by horizontal lines; b) AmB concentration (μg g^{-1}) in kidney, liver, spleen and brain. Statistical significant

differences: * = $p < 0.05$ AmB-GCPQ versus AmBisome®; c) Urea levels (mg dL^{-1}); d) Creatinine levels (mg dL^{-1}); e) Bilirubin levels (mg dL^{-1}); statistical significant differences: * = $p < 0.05$ AmBisome® vs infected control group; f) AST (U L^{-1}); f) ALT (U L^{-1}); f) Alkaline phosphatase (U L^{-1}); statistical significant differences: * = $p < 0.05$ AmB-GCPQ vs all the groups. Key: mouse 1 (-○-); mouse 2 (-Δ-); mouse 3 (-▽-); mouse 4 (- ◁ -); mouse 5 (-□-); mean (▬).